Astron. Astrophys. 351, 140–146 (1999)

ASTRONOMY AND ASTROPHYSICS

Starburst nuclei: ISO observations and models⋆

R. Siebenmorgen[1], **E. Krügel**[2], **and V. Zota**[2]

[1] ISO Data Centre, Astrophysics Division, Space Science Department of ESA, Villafranca del Castillo, P.O. Box 50727, 28080 Madrid, Spain
[2] Max-Planck-Institut für Radioastronomie, Auf dem Hügel 69, 53121 Bonn, Germany

Received 11 February 1999 / Accepted 4 May 1999

Abstract. *1.)* We present photometric data of three starburst galaxies (Mkn 496, Mkn 1116, NGC 6000) obtained with the Infrared Space Observatory (ISO) in the wavelength bands 2.5–11.6 μm (`P-40`) and 120–200 μm (`P-22`). In all galaxies, we detect the 9.7 μm silicate absorption feature and strong emission from PAHs; only the 3.3 μm band is below the sensitivity limit of the instrument. *2.)* We model the starbursts by computing the radiative transfer in the galactic nuclei under the assumption of spherical symmetry. By properly adjusting the distribution of stars and dust, we can fit the observed infrared radiation, including the PAH features. The dust is described by a mixture of large grains, very small grains and PAHs, the latter all of the same size (25 carbon atoms). The photo–destruction of the PAHs is computed in a physically consistent way. *3.)* We explore the parameter space by modeling the spectral energy distribution of the ultraluminous starburst galaxy Arp 220. Although the nucleus is deeply hidden by dust, the simple radiative transfer calculations allow an estimate of its global structure.

Key words: infrared: galaxies – galaxies: starburst – galaxies: nuclei – ISM: dust, extinction

1. Introduction

Star formation in external galaxies is intimately linked to questions concerning galaxy formation and evolution. Of particular interest are galaxies with star bursts. Because formation is taking place in interstellar clouds, the UV and optical stellar light is re–processed into infrared photons. The major part of the IR spectrum of starbursts is emitted from the nuclear region and the spectral energy distributions peak at about 100 μm. As their normalized spectra show similarities both in the mid infrared as well as in the far infrared (Rowan–Robinson & Crawford 1989, Roche et al. 1991), one may wonder whether starburst galaxies have a common structure.

The galactic nuclei are deeply hidden by dust so that it is necessary to observe at infrared wavelengths. Here the recent ISO mission (Kessler et al. 1996) gave new opportunities. Analyzing the data with radiative transfer models, one hopes to disclose some aspects of the true structure of the sources.

2. Observations

We undertook a photometric study of the IR emission of the three IRAS galaxies Mkn 496, Mkn 1116 and NGC 6000 with ISOPHT (Lemke et al. 1996). Observations include spectro–photometry in the wavelength range from 2.5 to 11.5 μm and far IR photometry between 120 and 200 μm using the observing templates P–40 and P–22 (Klaas et al. 1994). P–40 observations were performed with both detectors of the PHOT–S subsystem in triangular chopper mode. This mode implies chopping at two reference positions (OFF1, OFF2) and two ON–source measurements. An observing cycle consists of an OFF1–ON–OFF2–ON measurement scheme. The total on–source integration time is 512s. A chopper throw of $30''$ was adopted. We present P–22 observations of the C200 detector in filters at 120, 150, 180 and 200 μm, an integration time of 16s each, and rectangular chopping. We exclude P–22 chopped observations with the C100 detector because of yet unsolved technical problems. We mention that Mkn 496 = NGC 6090 had already been observed with ISO by Acosta–Pulido et al. (1996) and their C200 and P–40 spectra agree very well with ours.

Data were reduced with PIA (Version 7)[1]. The basic calibration steps are detailed in the ISOPHT Data User Manual (Laureijs et al., 1998). In addition, we smooth P–40 spectra by rebinning two neighboring points into one and color correct P–22 data by assuming a spectral shape $\nu^2 B_\nu(30\,K)$. The photometric uncertainty of P–22 chopped observations using PIA 7 calibration files is presently still large ($\sim$40%), but it is expected that the accuracy of the photometry will be improved once we better understand the detector and have up–dated calibration files.

Send offprint requests to: rsiebenm@iso.vilspa.esa.es

⋆ Based on observations with ISO, an ESA project with instruments funded by ESA Member States (especially the PI countries: France, Germany, the Netherlands and the United Kingdom) with the participation of ISAS and NASA.

[1] PIA is a joint development by the ESA Astrophysics Division and the ISOPHT Consortium led by the MPIA, Heidelberg. Contributing ISOPHT Consortium institutes are DIAS, RAL, AIP, MPIK, and MPIA.

Table 1. ISO chopped photometry with the C200 detector. All measurements have a signal–to–noise ratio greater than 10. The errors account for the large calibration uncertainty of ∼40%. Fluxes are color–corrected and in Jy.

Filter	Mkn 496	Mkn 1116	NGC 6000
120	12.3 ± 4.9	9.1 ± 3.6	61.5 ± 24.6
150	8.5 ± 3.4	7.0 ± 2.8	44.9 ± 18.0
180	6.1 ± 2.4	5.1 ± 2.0	30.6 ± 12.2
200	4.8 ± 1.9	3.7 ± 1.5	25.8 ± 10.3

3. Radiative transfer in galactic nuclei

Radiative transfer models for the disks and nuclei of galaxies have been carried out in various approximations by a number of authors (Krügel & Tutukov 1978, Efstathiou & Rowan–Robinson 1990, Spagna et al. 1991, Pier & Krolik 1992, Granato & Danese 1994, Krügel & Siebenmorgen 1994, henceforth KS94, Efstathiou & Siebenmorgen, 1995, Silva et al. 1998).

3.1. The source function

We compute the radiative transfer for the nucleus of the galaxy. The maps of nuclei generally appear at all wavelengths to first order round and therefore we feel justified to use for our crude endeavor models of spherical symmetry. The radiation transport code which we employ is detailed in KS94. Its potential was demonstrated by successfully modeling all relevant infrared data for the nucleus of M 82.

The crucial parameter in the transfer equation is the source function. For a dust cloud *without* distributed luminosity sources (like stars in a galactic nucleus) it reads

$$S_\nu(r) = \left[\varepsilon_\nu^{\rm d}(r) + J_\nu(r) \cdot \kappa_\nu^{\rm sca}\right] / \kappa_\nu^{\rm ext} \ . \quad (1)$$

The dust emission coefficient is given by

$$\varepsilon_\nu^{\rm d} = \kappa_\nu^{\rm abs} \int B_\nu(T)\, P(T)\, dT \ . \quad (2)$$

The absorption, scattering and extinction coefficient are denoted by $\kappa_\nu^{\rm abs}$, $\kappa_\nu^{\rm sca}$, $\kappa_\nu^{\rm ext}$, and the mean intensity of the interstellar radiation field by $J_\nu(r)$. The distribution function $P(T)$ in Eq. (2) equals the δ–function in the case of large grains because their temperature is constant. Then this equation just reads $\varepsilon_\nu^{\rm d} = \kappa_\nu^{\rm abs} B_\nu(T)$. For very small grains (such as PAHs) the function $P(T)$ has to be evaluated separately (see e.g. Siebenmorgen et al., 1992).

The model nuclei contain two kinds of stellar populations:

- Giants with 4000 K effective temperature, number density $n^{\rm G}(r)$ and spectral luminosity $L_\nu^{\rm G}$. They are very numerous and smoothly distributed and introduce into the source function the term $n^{\rm G}(r) \cdot L_\nu^{\rm G}$ which enters in the numerator of the right side of Eq. (1).
- OB stars from the starburst with an effective temperature of 30 000 K, number density $n^{\rm OB}(r)$ and luminosity $L^{\rm OB} = 10^5 {\rm L}_\odot$. Because they are so luminous, each immediate environment of an OB star presents a *hot spot* where the dust temperature has a local peak.

As was shown in KS94, when the luminosity of the galactic nucleus is dominated by OB stars, the hot spots have a great influence on the mid IR spectrum. The size of a hot spot follows from the condition that inside it, heating of the dust is dominated by the OB star, whereas outside heating by the interstellar radiation field $J_\nu(r)$ is more important. The emission from a hot spot, denoted by $L_\nu^{\rm hot}$, has to be computed in a special routine (for the original description see Krügel & Tutokov 1978) and is taken into account in the source function by the term $n_{\rm OB}(r) \cdot L_\nu^{\rm hot}$. Altogether, the source function of a galactic nucleus filled with stars is

$$S_\nu(r) = \frac{n_{\rm OB}(r) L_\nu^{\rm hot} + n^{\rm G}(r) L_\nu^{\rm G} + \varepsilon_\nu^{\rm d}(r) + J_\nu(r) \kappa_\nu^{\rm sca}}{\kappa_\nu^{\rm ext}} \ . \quad (3)$$

3.2. Dust model

We employ a dust model similar to that by Siebenmorgen & Krügel (1992). The large spherical grains have radii from 300 to 2400 Å with a size distribution exponent 3.5. They consist of silicate and amorphous carbon particles with a volume ratio $V_{\rm Si}/V_{\rm aC} = 1.4$. A fraction of 25% of the solid carbon is graphitic in the form of very small grains with radii from 10 to 20 Å and distribution exponent 4. Another fraction $Y_C^{\rm PAH}$ of the solid carbon is in PAHs. All PAHs have a skeleton of 25 C–atoms and 14 H–atoms at the periphery, corresponding to the maximum hydrogenation parameter for circular PAHs. Optical constants for silicate are from Laor & Draine (1993), for amorphous carbon (type BE) from Zubko et al. (1996), for graphite from Draine (1985), for the PAHs from Schutte et al. (1993). To minimize the number of free parameters in the fits, the dust model is kept constant and we only vary the abundance $Y_C^{\rm PAH}$ of the PAHs.

The dust–to–gas ratio is not required for computing the radiative transfer models. The total amount of dust in the galactic nuclei, $M_{\rm dust}$, follows from the visual extinction A_V and the dust radius $R_{\rm dust}$, as given in Table 2:

$$M_{\rm dust} \ = \ \frac{4\pi R_{\rm dust}^2 A_V}{3 K_V} \ . \quad (4)$$

Here it is assumed that the dust density ρ is constant, so $A_V = R_{\rm dust} \rho K_V$. The exact value of $M_{\rm dust}$ depends on the visual extinction coefficient K_V and thus on the particular dust model, but $K_V = 3 \cdot 10^4$ cm^2 per gram of dust (or $K_V = 200$ cm^2 per gram of gas) is a value that will not arouse much controversy.

3.3. Photodissociation of PAHs

In a strong UV radiation field, PAHs may evaporate. Although evaporation is not important for our objects, it was taken into account and treated by the following formalism details of which are found in Zota (1998). The photo–dissociation rate $k(U)$ of

Table 2. Parameters of the radiative transfer models.

Parameter	**Mkn 496**	**Mkn 1116**	**NGC 6000**	**Arp 220**
Distance	119 Mpc	100 Mpc	29.3 Mpc	73 Mpc
Luminosities				
OB–stars L_{OB}	$1.3 \cdot 10^{11} L_\odot$	$8 \cdot 10^{10} L_\odot$	$3.5 \cdot 10^{10} L_\odot$	$7.3 \cdot 10^{11} L_\odot$
Giants L_{giant}	$5 \cdot 10^{10} L_\odot$	$4 \cdot 10^{10} L_\odot$	$2 \cdot 10^{10} L_\odot$	$3.6 \cdot 10^{11} L_\odot$
Radius				
OB stars R_{OB}	150 pc	300 pc	200 pc	350 pc
Giants R_{giant}	800 pc	1100 pc	900 pc	1800 pc
Dust R_{dust}	1400 pc	1300 pc	1000 pc	1400 pc
Densities				
OB stars ρ_{OB}	$\propto r^{-2}$	$\propto r^{-1.5}$	$\propto r^{-2}$	const
Giants ρ_{giant}	$\propto r^{-1}$	$\propto r^{-1}$	$\propto r^{-1}$	$\propto r^{-1}$
Dust ρ_{dust}	const	const	const	const
Extinction				
A_V to center (r=0)	26.5 mag	27 mag	29 mag	54 mag
PAHs				
Y_C^{PAH}	0.01	0.015	0.012	0.01
Carbons n_C	25	25	25	25

the PAHs is described only by its internal energy U and the degrees of freedom s (see e.g. Forst 1973),

$$k(U) = k_0 \left(1 - \frac{E_0}{U}\right)^{s-1} \quad . \tag{5}$$

Despite this simplification, Jochims et al. (1996) achieved good agreement between dissociation measurements in the lab and a linearized version of Eq. (5) for small PAHs ($n_C < 25$) by properly choosing the fit–parameters k_0 and E_0. After Jochims et al. (1994), $E_0 \simeq 2.8$ eV and $k_0 = 10^{15} \ldots 10^{16}\ s^{-1}$ for the dissociation channels H, H_2 and C_2H_2. As typical emission rates for IR–photons are of order $10^2\ s^{-1}$, they suggest $k_{crit} \sim 10^2\ s^{-1}$ as the critical value for the onset of PAH dissociation. This corresponds after Eq. (5) to some internal energy U_{crit} and the latter is converted into an evaporation temperature T_{crit} by the canonical representation of the internal energy,

$$U_s(T) = \sum_{i=1}^{s} h\nu_i \left(\exp(h\nu_i/kT) - 1\right)^{-1} \quad . \tag{6}$$

The ν_i are the fundamental vibrations of the molecule; for small PAHs, these frequencies have been measured (e.g. Cyvin et al. 1979, Whitmer et al. 1978) or can be calculated. The effect of photo–ionization, which is the only competing reaction path for PAHs of high internal energy, stabilizes the PAHs against evaporation. This effect is accounted for in our models following Verstraete et al. (1990).

4. The models

4.1. Mkn 496, Mkn 1116 and NGC 6000

We first apply the radiative transfer code to the nuclei of Mkn 496, Mkn 1116 and NGC 6000. We attempt to reproduce in the models the infrared measurements which we obtained with ISOPHT, as well as IRAS and submm/mm data. Galactic nuclei have a diameter of only a few kpc, the active region being usually considerably smaller. Given the distance to our objects, the angular diameter of their nuclei on the sky is of order 10 arcsec, whereas the whole galaxies including their disks are some ten times bigger.

The luminosity in starburst galaxies is likely to be dominated by the nucleus. Therefore, when comparing theoretical fluxes of the nucleus with actual observations that were obtained with a beam larger than the nucleus, we assume that the contribution of the galactic disk is moderate. Qualitatively, one expects the disk to be more influential at submm wavelength because there must be plenty of interstellar matter in the disk. However, the star formation rate in the disk is probably relatively low.

The IR spectra are shown in Fig. 1 together with the fit results. The model fluxes refer to a uniform aperture (beam size) of 24″, about equal to the resolution of the `P-40` detector of ISO. The full lines in the right boxes of Fig. 1 show the overall fits. At far IR wavelengths, they are somewhat below our ISOPHT as well as the IRAS 100 μm points, but this is the way it should be for extended galaxies. The 1.3 mm fluxes of the two Markarians were obtained with an 11″ beam and lie therefore below the theoretical line.

In the left boxes, the P–40 spectra comprising the silicate absorption feature at 9.7 μm and the mid IR emission bands 6.2, 7.7, 8.6 and 11.3 μm are zoomed for easier read off. Overall, the models are not bad. However, the P–40 fluxes at 12 μm are generally smaller than the IRAS photometry at that wavelength. Assuming that IRAS is basically right, this may be due to a combination of several effects. For Mkn 496, the difference is marginal and may be fully explained by the broadness of the IRAS filter which includes part of the steeply rising spectrum beyond 12 μm. For NGC 6000, the difference is a bit larger. This galaxy is the nearest (29 Mpc) and its mid infrared emission may

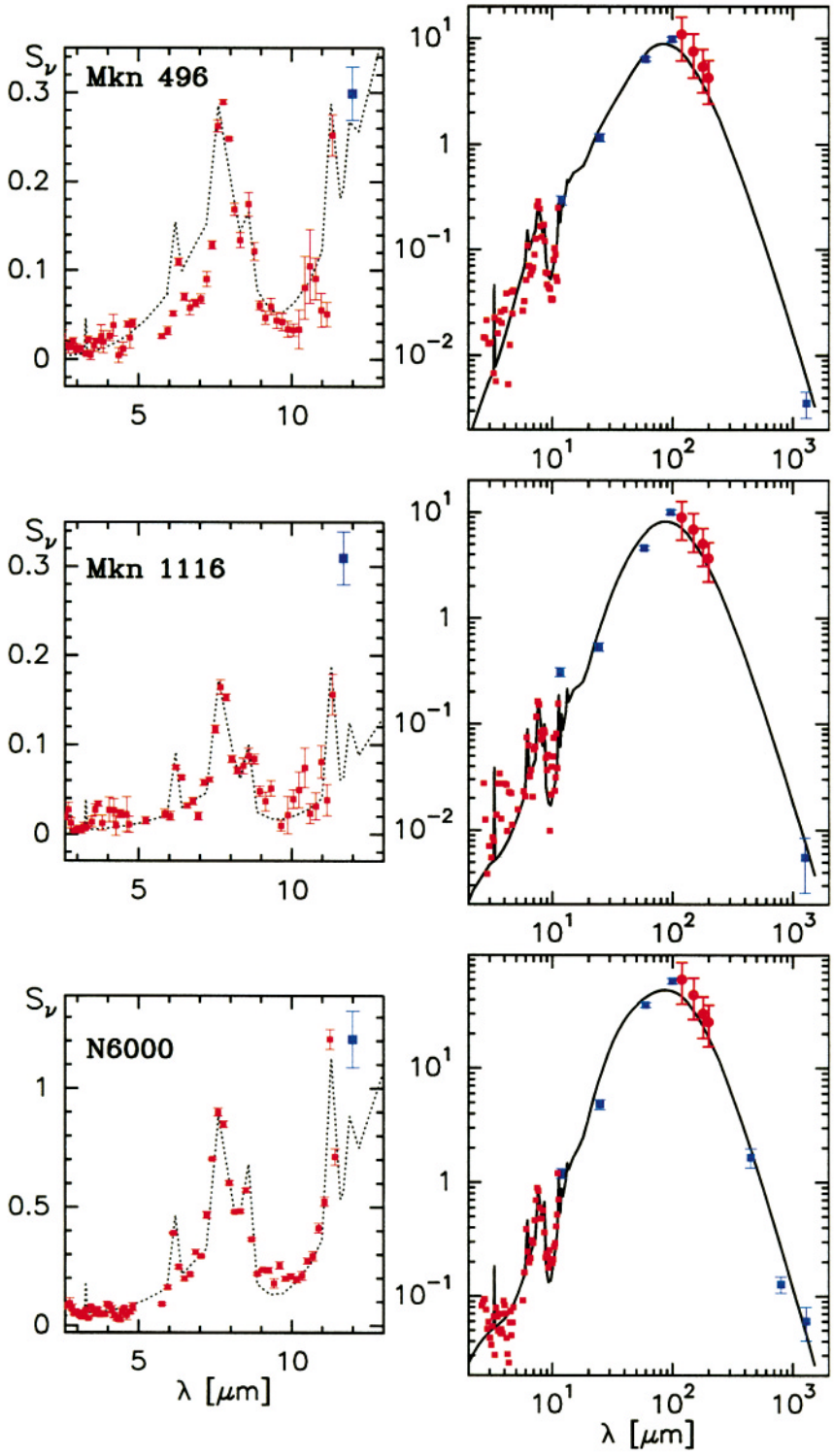

Fig. 1. Observations vs. radiative transfer models for the starburst galaxies Mkn 496, Mkn 1116 and NGC 6000. *Left:* Our `P-40` data and the 12 μm IRAS point (big square). *Right:* ISO photometry (circles), IRAS fluxes (squares). At 1.3 mm, the points for both Markarians refer to an 11″ beam (Chini & Krügel, priv. communication); for NGC 6000 at 1.3 mm to a 24″ beam and at the two submm wavelengths to ∼18″ beams (Chini et al. 1995). The models refer to a 24″ diaphragm.

be extended beyond the ISO beam (24″). Such radiation would still be picked up by IRAS which has a larger beam.

In Mkn 1116, the discrepancy amounts to a factor ∼2.5. Both previous effects may contribute. Moreover, the IRAS flux is close to the detection limit where there is always the tendency to overestimate the flux. But the most likely explanation lies in our observing position. We used IRAS coordinates, partly to be in line with the previous 1.3 mm continuum measurement, partly because it would not matter in the broad–beam P–22 observations. The IRAS position is 14″ off from the optical center. We therefore conclude that the P–40 and 1.3 mm fluxes towards the center of Mkn 1116 may be twice as large than those which we measured. The affect on the model parameters of Table 2 is, however, not dramatic. For example, to double

the mid IR fluxes of the model, one may just double the PAH abundance.

In all three galaxies, the 3.3 μm feature slipped detection because of ISOPHT's insufficient sensitivity. However, the model fluxes of this feature lie always within the observed noise. Unfortunately, there are no data to compare with our predictions for the 11.95 and 13.3 μm resonance.

The structure of the three nuclei is described in Table 2. All nuclei are powered by a starburst of $\sim 10^{11}\,L_\odot$ luminosity and there are about 10^6 OB stars within the central few hundred parsec. The nuclei are also similar otherwise: they have comparable total dust mass ($\sim 3\cdot 10^7\,M_\odot$), comparable extinction ($\sim$27 mag), size of the starburst region ($\sim$200 pc), and ratio of starburst to total luminosity ($\sim$2/3). The OB stars created in the burst have a strong central peak, their density increase is steeper than that of the giants ($n_{\rm OB}\propto r^{-2}$, whereas $n_{\rm G}\propto r^{-1}$). The OB star region, which is the place where the PAHs are excited and the mid IR radiation originates, has a moderate visual optical depth of $\sim$5 mag. Therefore most of the extinction occurs in the envelope of the galactic nucleus.

For illustration, the temperature profiles within the galactic nucleus of the large grains are plotted in Fig. 2. As the grains have a size distribution, there is at every radius r for each chemical component a range of temperatures. It is not a strict, but nevertheless quite general rule that if one has in a radiation field two grains of the same material and shape but different size, the smaller one is warmer. The upper boundary curve represents the smallest, the lower the biggest particles. The spread in temperature is much smaller in the outer parts of the galaxies because there the radiation field becomes very soft.

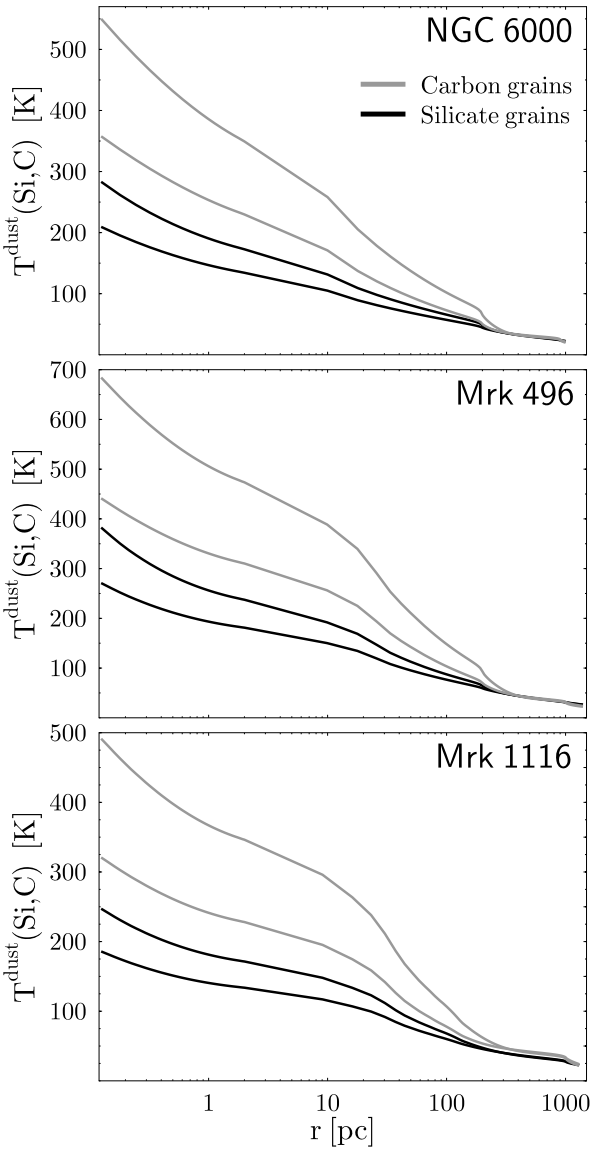

Fig. 2. Temperature of the large grains vs. galactic radius, separately for silicates and amorphous carbon grains. The upper curves refer to the smallest, the lower to the biggest grains.

4.2. Arp 220

To further illustrate the potential of modeling the IR spectra, we compute the radiative transfer for the nucleus of Arp 220. This is a famous ultraluminous object ($L\geq 10^{12}\,L_\odot$) which belongs to the local universe and is an order of magnitude brighter in the IR than the three galaxies discussed before.

Arp 220 is probably also powered by a starburst as, for example, Sturm et al. (1996) observe fine structure lines only of low excitation. These authors derive an optical depth $A_{\rm V}=50\pm 10$ mag. Their value is compatible with our model, also described in Table 2, which has a dust mass $\sim 7\cdot 10^7\,M_\odot$ within $r=1400$ pc.

Our model fits the IR emission quite satisfactorily (see Fig. 3). It correctly reproduces the 10 μm silicate absorption feature as well as the PAH resonances. The model fluxes are calculated for a 10″ beam; they therefore underestimate the submillimeter emission as Arp 220 is known to be more extended. The temperature profiles are shown in Fig. 4. They are flat within the starburst region as it should be for a constant density of the OB–stars (see Table 2). For comparison with another radiative transfer model which assumes a somewhat different geometry and includes optical emission from unobscured stars, one may consult Silva et al. (1998). As far as we can make out, except for this presence of stars outside the heavily veiled nucleus, there is no qualitative disagreement between their model and ours.

5. Discussion and conclusions

The interior of galactic nuclei is usually hidden to optical and near IR observers by a dust veil of high optical depth. Measurements in the far IR, which are not handicapped by obscuration, are until now always of low resolution and furthermore cannot detect stars directly. If one wishes to determine the spatial configuration of stars and dust in a galactic core, one has to use indirect means. One way is to model the observed IR energy distribution. If one succeeds in building a model that correctly reproduces the IR fluxes of a sufficiently large data base, one has, if not a true, but at least a self–consistent picture. If fur-

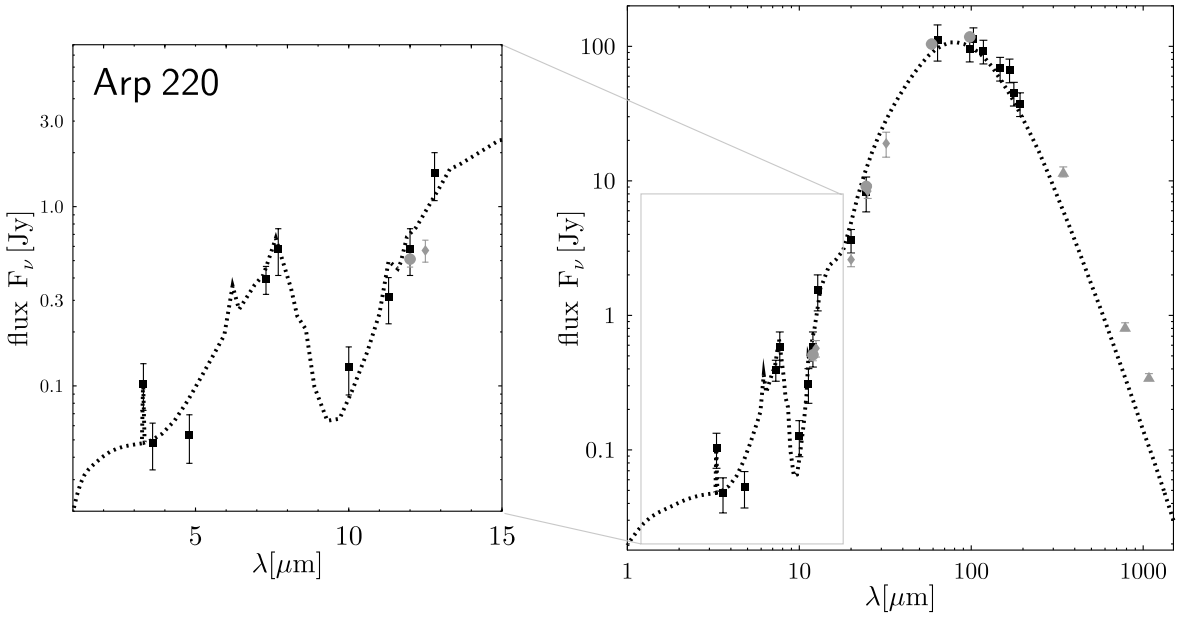

Fig. 3. Radiation transfer model of Arp220. ISOPHT (black squares, Klaas et al. 1997), IRAS (shaded circles), triangles (Rigopoulou et al. 1996), shaded diamonds (Wynn-Williams & Becklin 1993). The model (dotted line) refers to a $10''$ diaphragma.

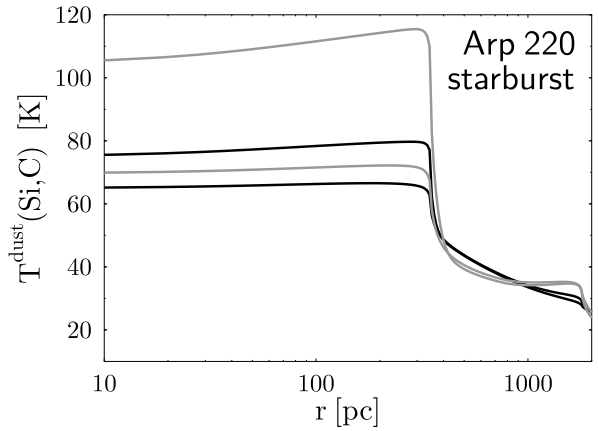

Fig. 4. Temperature of the large grains vs. galactic radius of Arp 220. Again the light lines refer to carbon grains, the fat one to silicates. See caption of Fig. 2.

thermore maps or observations of different spatial resolution indicate that spherical symmetry is not gravely violated, one has even derived the likely structure of the nucleus.

The data of the four galaxies for which we computed models are certainly not extensive, neither in spatial nor spectral resolution, and are therefore only a first step towards the goal. Nevertheless, the parameters in Table 2 give a first tentative description of the nuclei. Of course, because of the simplified geometry and the small number of parameters, one has to be skeptical about the uniqueness of the models. For example, one may wonder why the transfer code yields such a good fit to Arp 220. In the calculations, it was assumed that the OB star density is constant over a galactic radius of 350 pc, whereas one sees at 2.2 μm and 10 μm that this galaxy is a merger containing two nuclei separated by $1''$ or 350 pc (Graham et al. 1990, Miles et al. 1996). The real configuration is evidently not spherically symmetric. So the structure of the model is, of course, wrong on a scale $r < 400$ pc. But, on the other hand, the data which our model had to fit refer only to regions greater than $1''$. The more general result that most of the energy in Arp 220 comes from $r < 400$ pc and that this region has an optical depth $A_V \sim 14$ mag and that the total optical depth is about 50 mag are probably correct.

So the method of deriving the structure of an obscured galactic nucleus from modeling its observed IR emission by computing the radiative transfer is cheap and promising, if one does not forget its limitations.

Acknowledgements. Part of this work was kindly supported by the *Deutsche Forschungsgemeinschaft* under Project Number Kr 1110/5–1.

References

Acosta–Pulido J.A., Klaas U., Laureijs R.J. et al., 1996, A&A **315**, L121.

Chini R., Krügel E., Lemke R., Ward–Thompson D., 1995, A&A **295**, 317

Cyvin S.J. Cyvin B.N., Brunvoll J., et al., 1979, *Z. Naturforsch.* **34a**, 579

Draine B.T., 1985, ApJ Suppl. 57, 587

Efstathiou A., Rowan–Robinson M., 1990, MNRAS 245, 275

Efstathiou A., Siebenmorgen R., 1995, Models of dusty disks including transiently heated particles, in: ESO conference on "The role of dust in the formation of stars", eds.: H.U. Käufl and R. Siebenmorgen, Springer Berlin–Heidelberg–New York, 1996, ISBN – 3-540-61462-1

Forst W., 1973, *Theory of unimolecular Reactions*, Academic Press, New York
Graham J.R., Carico P., Matthews K., et al., 1990, ApJ 354, L5
Granato G.L., Danese L., 1994, MNRAS 268, 235
Jochims H.W., Rühl E., Baumgärtel H., Tobita S., Leach S., 1994, ApJ **420**, 307
Jochims H.W., Baumgärtel H., Leach S., 1996, A&A **314**, 1003
Klaas U., Krüger H., Heinrichsen I., Heske A., Laureijs R., *ISOPHT Observers Manual, Version 3.1* (1994) available at ISO Data Centre (http://www.iso.vilspa.esa.es)
Klaas U., Haas M., Heinrichsen I., Schulz B., 1997, A&A **325**, L21
Kessler M.F., Steinz J.A., Andregg M.E., et al., 1996, A&A 315, L27
Krügel E., Tutokov A.V., 1978, AA 63, 375
Krügel E., Siebenmorgen R., 1994, A&A **282**, 407
Laor A. & Draine B.T., 1993, ApJ 402, 441
Laureijs R.J., Klaas U., Richards R.J., Schulz B., 1998, "ISOPHT Data Manual" available at ISO Data Centre (http://www.iso.vilspa.esa.es)
Lemke D., Klaas U., Abolins J., et al., 1996, A&A 315, L64.
Miles J.W., Houck J.R., Hayward T.L., Ashby M.L.N., 1996, ApJ **465**, 191
Pier E.A., Krolik J.H., 1992, ApJ 401, 99
Rigopoulou D., Lawrence A., Rowan-Robinson M., 1996, MNRAS **278**, 1049
Roche P.F., Aitken D.K., Smith C.H., Ward M.J., 1991, MNRAS 248, 606
Rowan-Robinson M., Crawford J., 1989, MNRAS 238, 523
Schutte W.A., Tielens A.G.G.M., Allamandola L.J., 1993, *ApJ* **325**, 74
Siebenmorgen, R., Krügel, E., 1992, A&A, 259, 614
Siebenmorgen R., Krügel E., Mathis J.S., 1992, AA 266, 501
Silva L., Granato G.L., Bressan A., Danese L., 1998, ApJ 509, 103
Spagna G.F., Leung C.M., Egan M.P., 1991, ApJ 379, 232
Sturm E., Lutz D., Genzel R. et al., 1996, A&A **315**, L133
Verstraete L., Léger A., d'Hendecourt L., Dutuit O., Defourneau D., 1990, A&A **237**, 436
Whitmer J.C., Cyvin S.J., Cyvin B.N., 1978, *Z. Naturforsch.* **33a**, 45
Wynn–Williams C.G., Becklin E.E., 1993, ApJ **412**, 535
Zota V., 1998, *Modellierung der Infrarotstrahlung von Galaxienkernen unter Berücksichtigung von ISO–Beobachtungen*, PhD Thesis, University of Bonn
Zubko V.G., Menella V., Colangeli L., Bussoletti E., 1996, MNRAS 282, 1321